12.307
Project 1: Weather Extremes and Vortex Flow

John Marshall and Talia Tamarin-Brodsky*

Abstract

We study extreme vortices in the atmosphere associated with hurricanes and intense blizzards, and explore the dynamical principles that underlie their structure. First we set up a spinning vortex in our fluids laboratory using a rotating turntable. By changing the rate of rotation of the turntable, we can study the influence of rotation on the vortex and set up analogues of atmospheric vortices. Second, building on what we have learned we study the observed structure of intense cyclones and hurricanes using meteorological observations. The non-dimensional number that we use to connect the laboratory vortex to the atmospheric vortex, is known as the Rossby number, and is a measure of the importance of rotation on the vortex motion.

1 Background and introduction

Extreme weather is associated with intense wind systems that can be seen on daily weather maps: tropical cyclones, hurricanes, intense middle latitude cyclones and severe winter storms. For example, Fig.1 shows Category 5 Hurricane Maria which devastated the island of Dominica on the night of September 18, 2017 and was headed for landfall on the heavily populated island of Puerto Rico on September 20, 2017. At the same time, a weakening Hurricane Jose approached the New England coast as it transitioned into a nor'easter-like extratropical storm bringing severe weather to Boston.

As we shall see, all these systems are profoundly affected by the fact that the Earth is rotating. Such phenomena are able to concentrate Earth's spin in to local, extremely intense swirling wind patterns, which can have devastating impacts on coastal communities should they reach landfall.

*Notes originally developed by Lodovica Illari and John Marshall

Figure 1: Hurricanes Maria and Jose heading toward, respectively, Puerto Rico and New England, during September 2017.

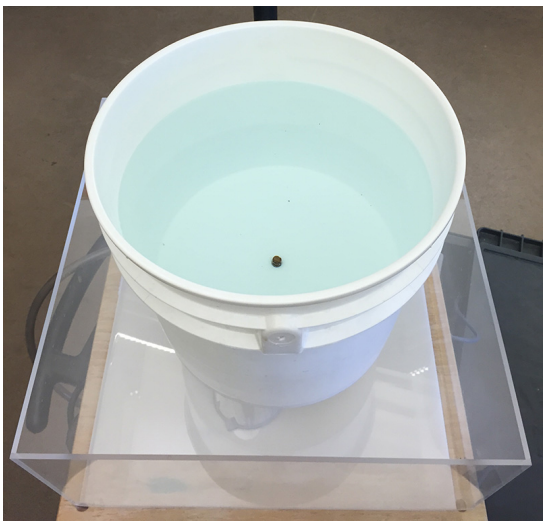

Figure 2: Apparatus used to create a fluid vortex in the laboratory. Water flows out through the hole at the center of a bucket which is rotating about its vertical axis. The bucket drains in to a tank which is seated on a rotating turntable.

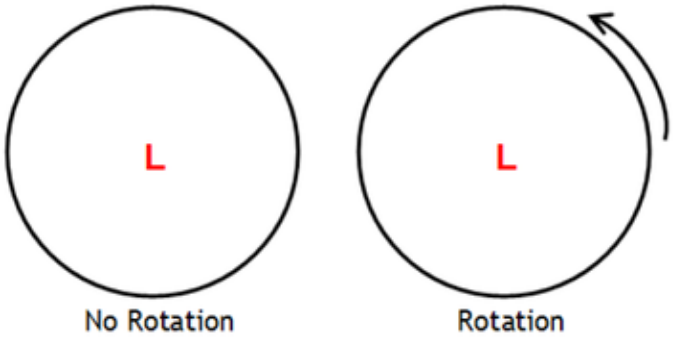

Figure 3: The bucket on the left is filled with water and sitting on the bench (and so not rotating) whereas the bucket on the right is on a turntable which is rotating counterclockwise. Sketch the expected trajectory of a particle of fluid as it exits from the hole at the center of the bucket, labeled L for 'low pressure'.

Let us consider how the timescale associated with the swirling wind patterns compares to that of the period of rotation of the Earth. We will define a non-dimensional number, $R_{timescales}$, a ratio of two time scales — the period of rotation of the Earth (or the rotating tank in our laboratory analogue) and the timescale of the vortex:

$$R_{timescales} = \frac{\text{rotation period of the Earth (or turntable)}}{\text{time scale of the flow}}. \tag{1}$$

If $R_{timescales} << 1$, then the time scale of the vortex is much longer than that of Earth's rotation period, and the dynamics is profoundly influenced by the rotation of the system. However, if $R_{timescales} >> 1$, then the timescale of the vortex is much shorter than Earth's rotation period, and rotation is not important.

We now introduce some of the ideas in the following simple, but highly instructive laboratory experiment. A bucket of water with a hole in the middle but with a stopper in place to keep the water escaping (as shown in Fig.2), is placed on a rotating turntable. Upon unplugging the hole, water exits from the bucket setting up a pressure gradient with low pressure at the center denoted by the 'L' in Fig.3, and higher pressure on the periphery. This pressure gradient force is directed radially. Sketch the trajectory of a water parcel as it exits from the bucket when the bucket is not rotating and when the bucket is rotating.

1.1 Setting up a vortex in the laboratory

We are now going to carry out the experiments that you just visualized and see whether your predictions are correct! The apparatus comprises a plastic cylinder – a bucket — filled most of the way with water and with a stoppered hole in the center. We consider two cases,

one in which the bucket is on a bench (and so not rotating) and one in which the bucket is on a turntable, spinning in an anticlockwise direction to represent the turning of the Earth. Once the hole is unplugged, a pressure gradient will develop with lower pressure over the hole thus driving the water out of the bucket. Our goal is to note the trajectories of water parcels as they exit the tank and to calculate $R_{timescales}$, given by Eq.(1), at 3 different radii.

For each trial, we release a paper dot:

1. near the outer rim of the bucket (but not touching the edge),
2. at an intermediate radius,
3. close to the center.

What is the trajectory of particle in the two trials, and how does it compare to your predictions?

Note how, in the rotating case, water flows inward toward the axis of rotation acquiring an anticlockwise swirling motion which gets more and more vigorous as it approaches the center of the cylinder. Can you figure out why this happens?

Using your stopwatch and the video monitor, estimate the time it takes the paper dot to complete one revolution — we can use this as an estimate of the 'timescale of the motion'. Take note of the rotation rate of the rotating table and from this compute the period of rotation.

We estimate $R_{timescales}$ from Eq.(1) at three different radii:

$$R_{timescales\_outer} = ...$$
$$R_{timescales\_middle} = ...$$
$$R_{timescales\_center} = ...$$

Where is $R_{timescales}$ large, small, and order unity? What does this tell us about the varying influence of rotation across the vortex?

Notice how the surface of the water plunges down toward the center of the cylinder resulting in a pressure gradient force directed radially inward. What outward force is balancing this inward pressure gradient force?

In the laboratory component of Project 1, which we now describe, we will carry out a more sophisticated version of the above experiment in which a balanced vortex is set up and explored in detail. We will develop some theory to go along with it which will help us interpret meteorological observations of intense vortices.

2 Fluid laboratory: Radial inflow experiment

2.1 Experimental procedure

The laboratory experiment — known as 'radial inflow' or 'balanced vortex' — is a more controlled, perpetual motion version of the 'hole in a bucket' experiment just described. We rotate a cylinder about its vertical axis, as shown in Fig.4; the cylinder has a circular drain hole in the center of its bottom. Water enters at a constant rate through a diffuser on its outer wall and exits through the drain. The water is then pumped back around enabling a steady state to be achieved. The system is viewed from above by a camera which is rotating with the turntable — i.e. in the rotating frame of reference.

When the apparatus is rotating the water acquires a pronounced swirling motion as it exits the tank: fluid parcels *spiral* inward as sketched in Fig.5 (rhs). Even at modest rotation rates of $\Omega = 1$ radian per second (corresponding to a rotation period of around 6 seconds)[1], the effect of rotation is marked and parcels complete many circuits before finally exiting through the drain hole. In the presence of rotation the free surface becomes markedly curved, high at the periphery and plunging downwards toward the hole in the center. When the apparatus is not rotating, particle trajectories are less distinctive but are generally directed radially inward (as sketched in Fig.5, lhs) and the free surface is observed to be rather flat.

2.2 Measurements and experimental procedure

The main objective of our experiment is to measure, and interpret in terms of mechanics and angular momentum principles (see theory below), the flow field and its dependence on rotation rate. We will also think about the relation between the flow field and the pressure field, given by the height of the free surface. This can exhibit pronounced curvature, diving down toward the hole in the middle, particularly in the case of higher rotation rates.

We carry out three experiments, one at low rotation rates (1rpm), medium (6rpm) and high (rpm) — don't try and break the apparatus by making it fly off the table!

In each experiment we:

1. record data from the overhead camera, rotating with the turntable, showing the position of particles as a function of time using the particle tracker provided,

2. plot trajectories of chosen particles (using Excel or Matlab, or your program of choice),

[1]Note that if Ω is the rate of rotation of the tank in radians per second, then the period of rotation is $\tau_{\rm tank} = \frac{2\pi}{\Omega}$. Thus if $\tau_{\rm tank} = 2\pi s$, then $\Omega = 1$.

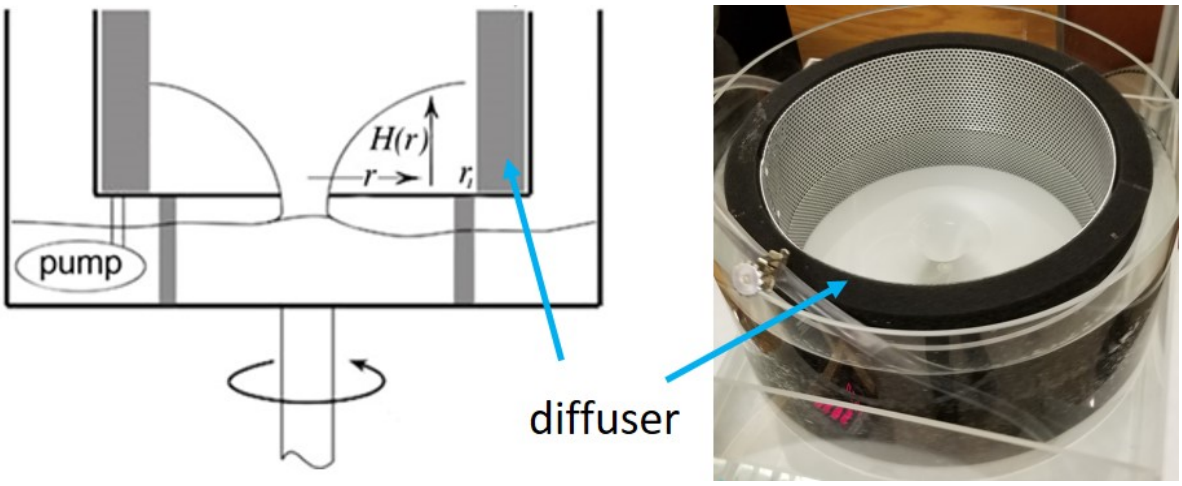

Figure 4: The radial inflow apparatus. A cylindrical diffuser is placed in a larger tank and used to produce an axially symmetric, inward flow of water toward a drain hole at the center. Below the tank there is a large catch basin, partially filled with water and containing a submersible pump whose purpose is to return water to the diffuser in the upper tank. The whole apparatus is then placed on a turntable and rotated in an anticlockwise direction. The path of the fluid is visulised by tracking paper dots on the free surface.

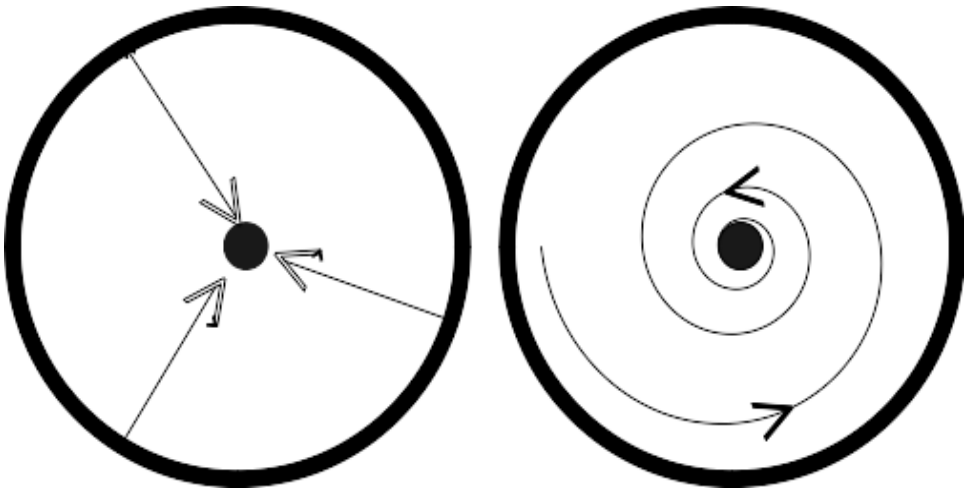

Figure 5: Idealized flow patterns (left) in the absence of rotation and (right) when the apparatus is rotating in an anticlockwise direction.

Figure 6: Trajectory of a particle in the rotating frame as it circulates around in the swirling vortex.

3. compute particle velocities as a function of radius,

4. plot the Rossby number, defined in Eq.(12) below, as a function of radius,

5. interpret in terms of the prediction from theory, Eq.(14), presented below.

Measuring position and velocity of particles. We record a sequence of images using the overhead camera and deploy particle tracking software on the laboratory computers to track chosen particles. An example is shown in Fig.6. This returns the coordinates of individual particles as a function of time (frame number). From this we can compute both the azimuthal (v_θ) and radial (v_r) velocity of the particles in the rotating frame of reference, using a cylindrical coordinate system — see Fig.7.

From this data we can test whether the azimuthal speed of the dots, $v_\theta(r)$, is consistent with angular momentum conservation, Eq.(4) below. We can also compute how the Rossby number, given by Eq.(12), varies across the vortex. This can be compared to the theoretical prediction, Eq.(14), that would pertain if the particles did indeed conserve angular momentum. This radial distribution of Rossby number will be a quantity that we compute from meteorological observations in the 'atmospheric data' component of our project.

Tips on how to use the particle tracker and how one converts from Cartesian to cylindrical coordinates (so as to compute, for example, $v_\theta(r)$) can be found on our course website.

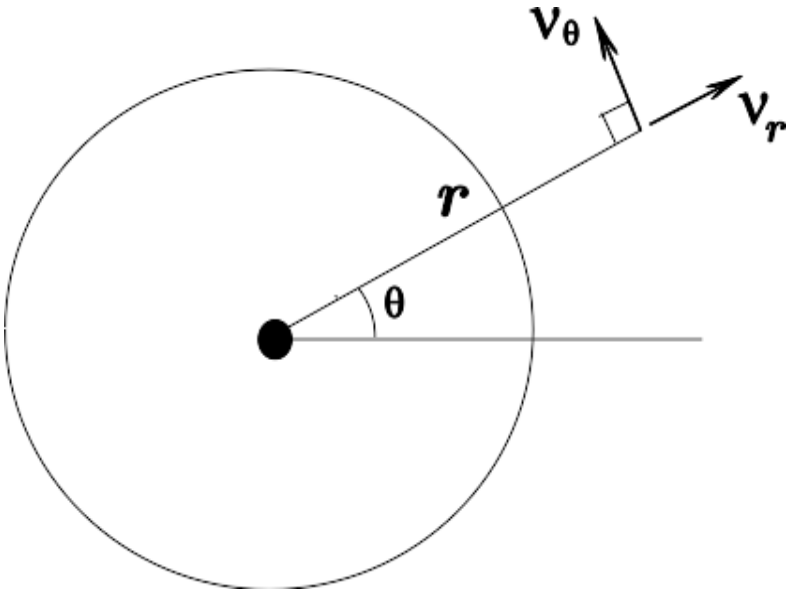

Figure 7: The velocity of a fluid parcel viewed in the rotating frame of reference: $v_{rot} = (v_r, v_\theta)$ in radial and azimuthal directions, (r, θ) coordinates.

2.3 Theory of a balanced vortex

Frames of reference. If V_θ is the azimuthal velocity in the absolute frame (the frame of the laboratory) and v_θ is the azimuthal speed *relative* to the tank (measured using the camera co-rotating with the apparatus) then (see Fig.7):

$$V_\theta = v_\theta + \Omega r, \tag{2}$$

where Ω is the rate of rotation of the tank in radians per second. Note that Ωr is the azimuthal speed of a particle fixed to the tank at radius r from the axis of rotation.

Angular momentum. Fluid entering the tank at the outer wall will have angular momentum because the apparatus is rotating. At r_1, the radius of the diffuser, fluid has azimuthal velocity Ωr_1 and hence angular momentum Ωr_1^2. As parcels of fluid flow inwards axi-symmetrically toward the central hole, they might be expected to conserve this angular momentum (provided that they are not rubbing against the bottom or the side, so that we may ignore friction). Conservation of angular momentum states that:

$$V_\theta \; r = \text{constant} = \Omega r_1^2. \tag{3}$$

Here V_θ is the azimuthal velocity in the laboratory (inertial) frame given by Eq.(2). Combining Eqs.(3) and (2) we find that the azimuthal speed in the rotating frame is:

$$v_\theta = \Omega \frac{(r_1^2 - r^2)}{r} \ . \tag{4}$$

Thus $v_\theta = 0$ at $r = r_1$ and v_θ increases as r decreases. We can readily test this prediction against the observations of trajectories obtained in the laboratory using the particle tracker.

We now consider the balance of forces in the vertical and radial directions, expressed first in terms of the absolute velocity V_θ and then in terms of the relative velocity v_θ.

Vertical force balance. We suppose that the pressure at any depth in the fluid is set by the weight of water above that level[2]:

$$\underbrace{p}_{\text{force/unit area}} = -\underbrace{\rho z}_{\text{mass/unit area}} \times \underbrace{g}_{\text{gravity}} + \text{const}$$

where ρ is the (constant) density, g is the acceleration due to gravity and z is a vertical coordinate increasing upwards (from $z = 0$ at the base of the tank). Note the minus sign ensures that pressure decreases on going upwards. At the free surface, at height $H(r)$ from the bottom, we suppose that the pressure vanishes (actually p = atmospheric pressure at the surface, which can be taken as zero). Thus, we have:

$$p(r, z) = \rho g \left(H(r) - z \right). \tag{5}$$

At the bottom $p = \rho g H$ and p decreases linearly to zero at the free surface where $z = H$.

Radial force balance in the non-rotating frame. If the pitch of the spiral traced out by fluid particles is tight (*i.e.* in the limit that $\frac{v_r}{v_\theta} << 1$, appropriate when Ω is sufficiently large) then the centrifugal force directed radially outwards acting on a particle of fluid is balanced by the pressure gradient force directed inwards associated with the tilt of the free surface. This radial force balance can be written in the non-rotating frame thus:

$$\underbrace{\frac{V_\theta^2}{r}}_{\text{Centrifugal acc}^{\text{n}}} = \underbrace{\frac{1}{\rho}\frac{\partial p}{\partial r}}_{\text{pressure gradient}} \ .$$

[2]The differential form of this relation is:

$$\frac{\partial p}{\partial z} + \rho g = 0$$

which is known as 'hydrostatic balance', the pressure distribution that pertains in a resting fluid.

Figure 8: The free surface of a fluid in solid body rotation takes up a parabolic shape, as can be seen in this large square tank of water rotating at 20rpm.

Using Eq.(5), the radial pressure gradient force in the above can be directly related to the gradient of the free surface enabling the force balance to be written:

$$\frac{V_\theta^2}{r} = g\frac{\partial H}{\partial r}. \tag{6}$$

Radial force balance in the rotating frame. Using Eq.(2), we can express the centrifugal acceleration in Eq.(6) in terms of velocities in the rotating frame thus:

$$\frac{V_\theta^2}{r} = \frac{(v_\theta + \Omega r)^2}{r} = \frac{v_\theta^2}{r} + 2\Omega v_\theta + \Omega^2 r \tag{7}$$

Hence our radial momentum balance becomes

$$\frac{v_\theta^2}{r} + 2\Omega v_\theta + \Omega^2 r = g\frac{\partial H}{\partial r}. \tag{8}$$

Solid body rotation state. Note that if the water in the tank is at rest in the rotating frame of reference, i.e. $v_\theta = 0$ in Eq.(8) (this in known as solid body rotation) then

$$\frac{\partial H_{\text{solid body}}}{\partial r} = \frac{\Omega^2 r}{g} \text{ and so } \; H_{\text{solid body}} = H_{r=0} + \frac{\Omega^2 r^2}{2g}, \tag{9}$$

where $H_{r=0}$ is the height of the water at $r = 0$ in the solid body rotation state. Note that the free surface in the solid body rotation state has a parabolic form. The surface is tilted in the steady state because the inward acceleration due to the tilt of the free surface ($g\frac{\partial H}{\partial r}$) is exactly balanced by the centrifugal acceleration directed outward $\Omega^2 r$. See Fig.8

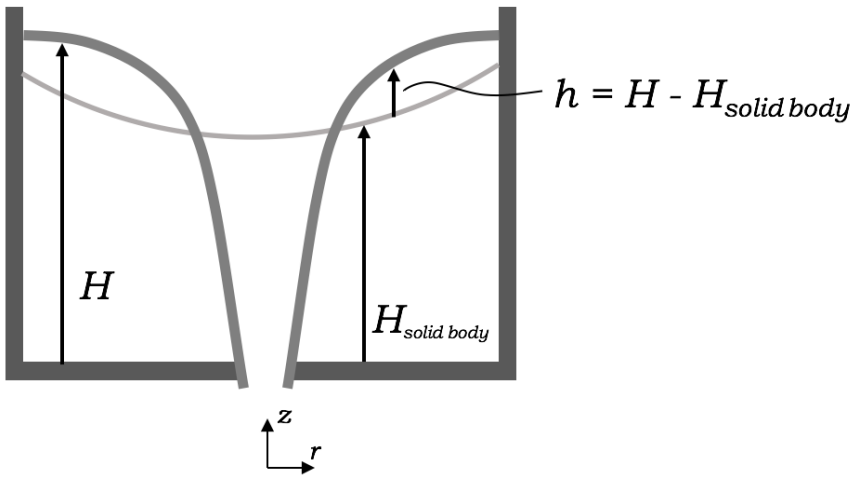

Figure 9: Height of the free surface, h, relative to solid body: $h = H - H_{\text{solid body}}$. H is the actual height of the free surface

The Rossby number and geostrophic balance. Eq.(8) can be simplified by writing $\Omega^2 r = \frac{\partial}{\partial r}\left(\frac{\Omega^2 r^2}{2}\right)$ and defining a quantity h:

$$h = H - H_{\text{solid body}} = H - \frac{\Omega^2 r^2}{2g}, \tag{10}$$

the height of the free surface measured relative to that of the reference parabolic surface, using Eq.(9) — see Fig.9. Then Eq.(8) can be written in term of h thus:

$$\frac{v_\theta^2}{r} = g\frac{\partial h}{\partial r} \underbrace{-2\Omega v_\theta}_{\text{Coriolis acc}^{\text{n}}} : \qquad \text{gradient wind balance} \tag{11}$$

This balance of forces is known as 'gradient wind balance'.

Eq.(6) and Eq.(11) are completely equivalent statements of the balance of forces. The distinction between them is that the former is expressed in terms of V_θ, the latter in terms of v_θ. Note that Eq.(11) has the same form as Eq.(6) except:

1. an extra term, $-2\Omega v_\theta$, appears on the rhs of Eq.(11) — this is called the 'Coriolis acceleration'. It has appeared because we have chosen to express our force balance in terms of *relative*, rather than absolute velocities.

2. the pressure gradient force is expressed in term of h (the height measured relative to the reference parabolic surface) rather than H.

Let us compare the magnitude of the centrifugal acceleration, $\frac{v_\theta^2}{r}$, and the Coriolis accel-

eration, $2\Omega v_\theta$, terms in Eq.(11). Their ratio is the 'Rossby number'[3]:

$$R_o = \frac{|v_\theta|}{2\Omega r} \tag{12}$$

If $R_o << 1$, the $\frac{v_\theta^2}{r}$ term can be neglected in (11). In this limit, Coriolis and pressure gradient terms balance one another.

$$g\frac{\partial h}{\partial r} - 2\Omega v_\theta = 0: \quad \text{geostrophic balance} \tag{13}$$

Equation (13) is a simple form of the 'geostrophic equation' relating velocities in the rotating frame to the horizontal pressure gradient in the limit of small R_o.

How large is R_o in our experiment? We can estimate its size by computing v_θ based on angular momentum conservation. Using the angular momentum conserving prediction (4) in (12) we find, for this profile,

$$R_o = \frac{1}{2}\left(\left(\frac{r_1}{r}\right)^2 - 1\right). \tag{14}$$

Thus $R_o = 1$ at $r = r_1/\sqrt{3}$; $R_o < 1$ if $r > r_1/\sqrt{3}$ (the region of geostrophic balance) and so, in the outer regions of the flow, the inward radial pressure gradient is balanced by outward Coriolis forces (small R_o): the flow is in geostrophic balance here. In the inner regions, $r < r_1/\sqrt{3}$, $R_o > 1$. But as parcels spiral into the drain they pass through a region where R_o becomes increasingly large and v_θ^2/r in Eq.(11) becomes a dominant term. In the limiting case $R_o \gg 1$, the centrifugal term dominates the Coriolis term in Eq.(11), and we have what is known as "cyclostrophic balance:"

$$\frac{v_\theta^2}{r} = g\frac{\partial h}{\partial r}: \quad \text{cyclostrophic balance} \tag{15}$$

Non-dimensional expressions. When making connections between the real world phenomena and laboratory abstractions (e.g. the flow in a hurricane and our laboratory vortex), it is useful to make use of non-dimensional numbers such as the Rossby number. If we non-dimensionalize distance by r_1 and velocity by Ωr_1 (the speed that a particle has as it exits

[3]It is interesting to compare the Rossby number defined here with the ratio of timescales $R_{timescales}$ written down in Eq.(1) and used in our initial exploration of our laboratory vortex:

$$R_{timescales} = \frac{2\pi/\Omega}{2\pi r/v_\theta} = \frac{v_\theta}{\Omega r} = 2 \times R_o.$$

Thus $R_{timescales}$ is exactly twice the Rossby number. The two non-dimensional numbers are essentially equivalent to one another, apart from the numerical factor of 2.

from the diffuser) then we may define non-dimensional distance and speed thus:

$$\widetilde{r} = \frac{r}{r_1},\ \widetilde{v_\theta} = \frac{v_\theta}{\Omega r_1}.$$

Then Eqs.(4 & 14) can be written:

$$\widetilde{v_\theta} = \frac{(1-\widetilde{r}^2)}{\widetilde{r}};\quad R_o = \frac{1}{2}\left(\left(\frac{1}{\widetilde{r}}\right)^2 - 1\right) \tag{16}$$

Thus $\widetilde{v_\theta}$ and R_o only depend on $\widetilde{r}$ and not on Ω! Is this true of the data you analyze in the radial flow experiment?

We will see that the range of Rossby numbers in our laboratory vortex — from large in the center to small on the periphery — are very similar to those found in Hurricanes and strong vortices on Earth, suggesting that the dynamical balances in the latter are the same as captured in our laboratory.

3 Vortices in the atmosphere

We will make use of what we have learned about the nature of laboratory vortices in rotating systems to explore atmospheric vortices using atmospheric data. Just as in our study of laboratory vortices, the Rossby number will be the key non-dimensional number that threads through our exploration. We begin by estimating the Rossby number in atmospheric vortices on large and small scales.

3.1 Examples of intense atmospheric vortices on large and small scales

The atmosphere is full of swirling wind patterns which often comprise intense vortex structures, as can be seen in Fig.10, a global IR satellite image of clouds on Feb 11, 2019. We observe vortical patterns of varying sizes, from large ones with scales of thousands of kilometers to small-scale vortices within which are embedded intense convective clouds clusters and thunderstorms. Tornadoes, which have a scale of only few km, can often develop in regions of severe thunderstorms, but are too small to be seen in such global images.

Many types of atmospheric vortices exist, which can be organized as a function of scale, from large to small, as listed below:

The Jet Stream (scale = 3000km): a current of fast-moving winds at the height of 10km or so, flowing from west to east around a low pressure area located over the cold polar regions. It is sometimes called the "Polar Vortex" — see Fig.11 and accompanying video. A similar jet stream flows around the South Pole.

Blizzards (scale = 1000km) — winter snow storms associated with strong winds circulating anti-clockwise around a low pressure center. They tend to develop along the "Polar Front", a mid-latitude region of strong temperature gradient, marking the boundary between cold polar air and warm tropical air — see Fig.12.

Hurricanes (scale = few 100skm): — tropical storms associated with very strong winds circulating anti-clockwise around a very low pressure center, the 'eye' of the hurricane. Hurricanes are fueled by energy in warm surface waters of the ocean and tend to occur in the summer/fall season — see Fig.13.

Tornados (scale = 1km) — small-scale vortices with extremely strong, damaging winds, which can develop out of strong thunderstorms — see Fig.14. In a tornado the air can swirl either clockwise or anti-clockwise.

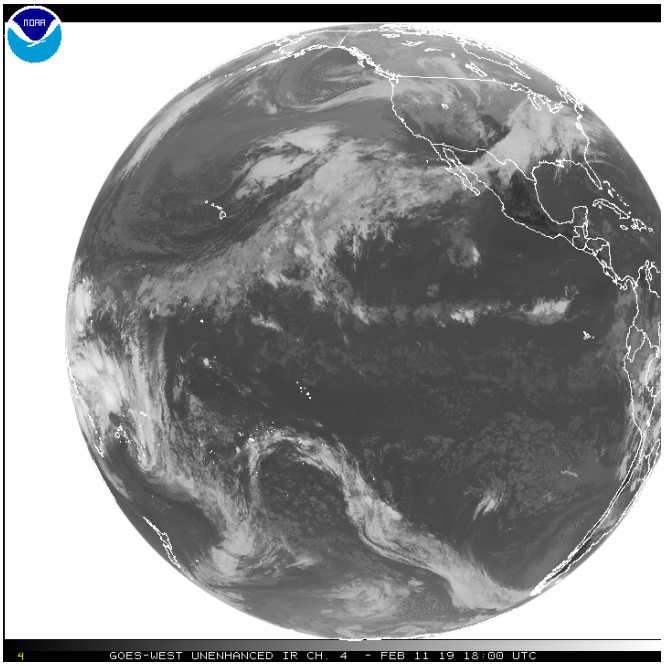

Figure 10: A global satellite image of Earth from Feb 11, 2019. The white areas are clouds and the darker areas clear sky. You can view an accompanying movie loop here: https://www.goes.noaa.gov/dml/west/fd.

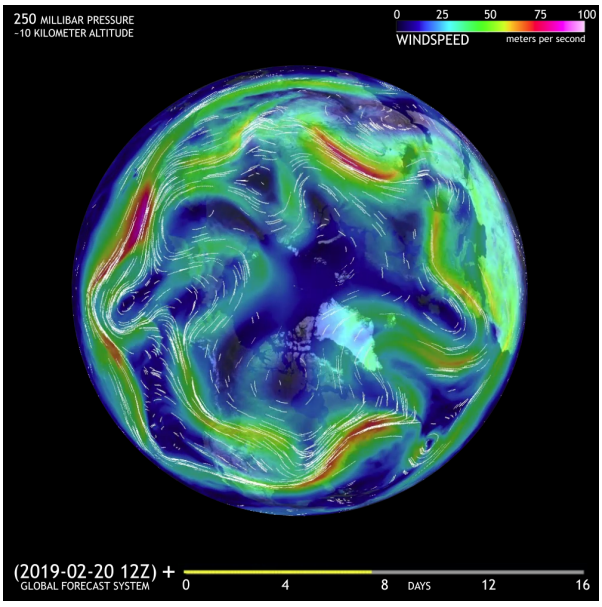

Figure 11: The jet stream at 250 HPa (at a height of, roughly, 10km) as seen on Feb 20, 2019. The areas shaded in red correspond to wind speeds that exeed 50ms^{-1}. The jet stream is in constant motion, as the 'ribbon' of intense winds undulates north and south, as can be seen in the accompanying movie.

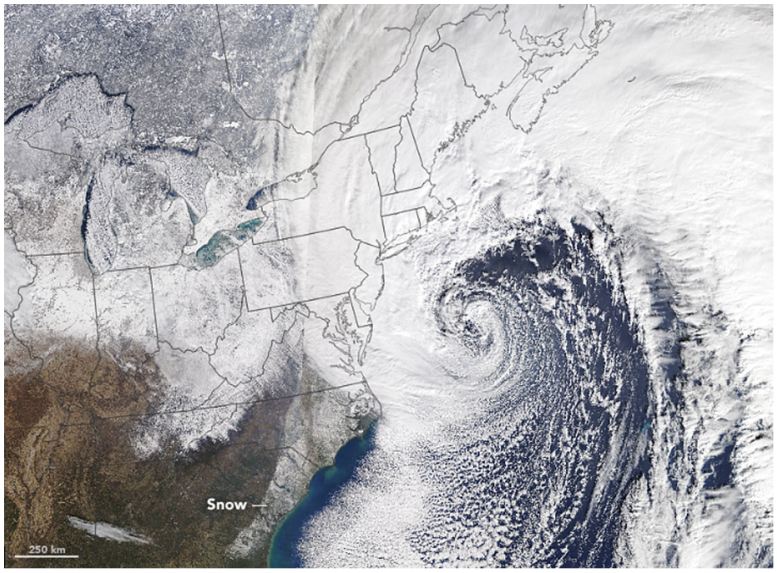

Figure 12: A satellite image of clouds showing the system that brought the blizzard of January 4, 2018 to the east coast. We see cold air moving down from the Arctic on the west of the system and warm air moving up from the tropics on the east — for more see: https://www.weather.gov/okx/Blizzard_Jan42018.

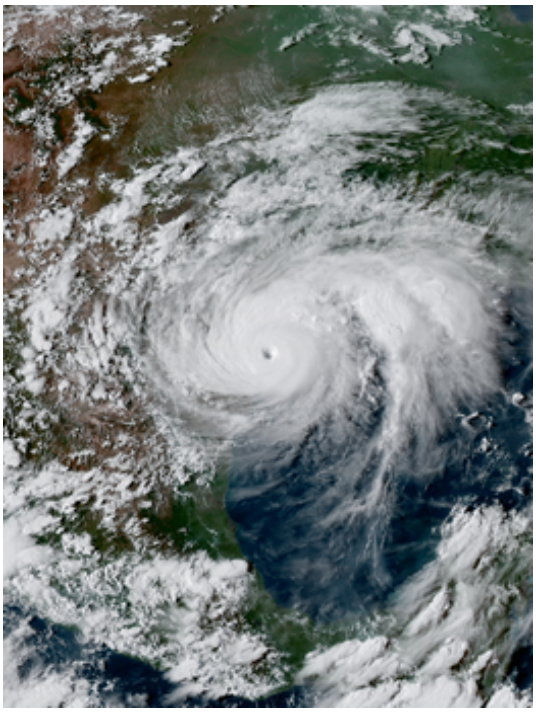

Figure 13: Hurricane Harvey (category 5) which reached landfall on the coast of Texas on August 25, 2017 — for more see: https://earthobservatory.nasa.gov/images/90822/hurricane-harvey-approaches-texas

Figure 14: A tornado in Iowa on July 19, 2018, one of 19 tornadoes that developed over the central planes. For more see: https://www.weather.gov/dmx/20180719_Tornadoes.

3.2 Estimating the Rossby number as a function of scale

We will now estimate the Rossby number of various atmospheric vortices, in a manner which is exactly analogous to that used in our laboratory experiments in Section 1.1. Rather than using paper dots, we will launch 'virtual' particles in to the evolving wind patterns using the EsGlobe, an interface for displaying and interacting with data — 12.307 website.

Planetary scale – the jet stream. Use the EsGlobe particle tracking interface to explore how long it takes for a parcel of air in the jet stream to circumnavigate the globe (set level = 10km $\sim$ 250 mb, where the jet speed typically reaches a maximum). Estimate the $R_{timescales}$ (as a ratio of time scales) defined by Eq.(1). Note that the Rossby number, Eq.(12), is given by $R_o = \frac{1}{2} R_{timescales}$ for an axi-symmetric vortex (see footnote on page 11). Is the Rossby number large or small and what does that tell us about the balance of forces that maintains the jet stream?

Mid-latitude cyclones — blizzards and Nor'easters. How long does it take for a parcel of air associated with a blizzard (or a mid-latitude cyclone) to travel full circle around the low pressure center? Use the same trajectory interface but set level = 5km, $\sim$ 500 mb, the level that sets the speed of propagation of mid-latitude cyclones. Again, estimate the Rossby number and discuss the typical balance of forces in a large-scale blizzard.

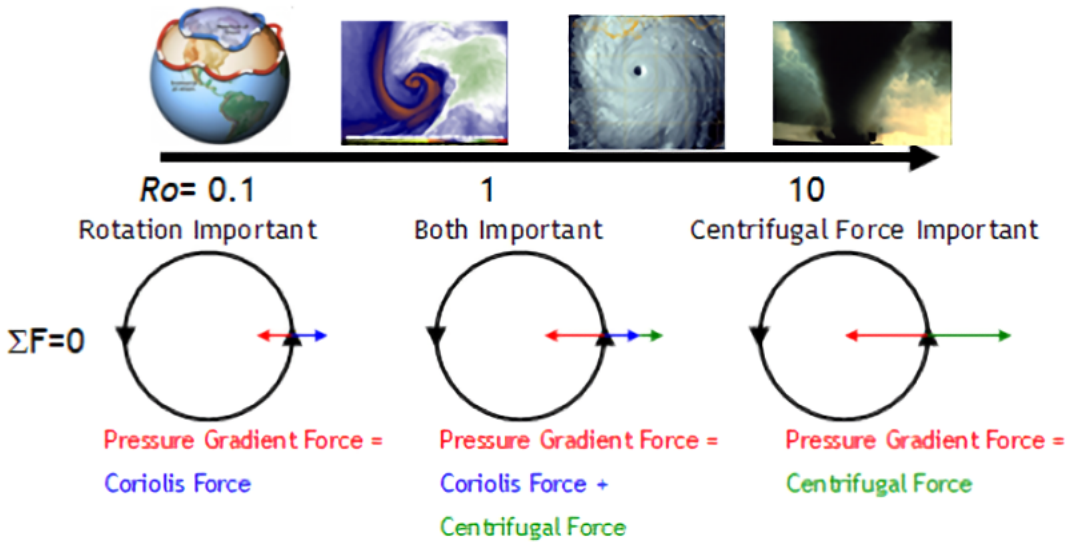

Figure 15: Significance of Rossby number as it relates to the balance of forces in vortices of different scales. On the planetary scale (lhs) $R_o << 1$ and pressure gradient forces are balanced by Coriolis forces. On the scale of a tornado (rhs) $R_o >> 1$ and pressure gradient forces are balanced by centrifugal forces.

Tropical cyclones — hurricanes. Repeat the same procedure but for hurricane Harvey (August, 2018). Use the Harvey winds available from the EsGlobe interface and set level = 1km , $\sim$ 850 mb, the level at which hurricane winds are the strongest. Estimate the Rossby number and discuss the typical balance of forces for a hurricane.

What about a tornado? Discuss the likely balance of forces.

In summary you should find that R_o depends on scale, broadly as sketched in Fig.15. On the large-scale, $R_o << 1$, and the dynamics is dominated by Earth's rotation, i.e. the Coriolis force. In this case the dominant radial force balance is given by Eq.(13). In contrast, if $R_o >> 1$, then centrifugal forces acting on the fluid parcel are dominant. In this case the dominant radial force balance is given by Eq.(15). In each of these cases, the force directed radially-outwards from the center of the vortex (whether Coriolis or centrifugal) is balanced by the pressure gradient force directed inwards, toward the low pressure at the center.

3.3 Jet stream in Geostrophic balance

Use the EsGlobe Atmospheric climatology interface to plot the zonal component of the wind field at 250mb, together with the height of the 250mb surface. An example is shown in Fig.16 from a January climatology. The globe has been orientated so that the north pole (NP) is at the center of the plot. Note:

1. the wind blows from west to east, circling cyclonically (anti-clockwise, looking down from the NP) around the pole. The reddest areas are the fastest, reaching speeds of 50ms^{-1} or so.

2. the 250mb surface is low over the pole (a height of 9600m or so) and gently rises moving in to the tropics (to a height of 10800m or so).

3. since $R_o << 1$, the zonal flow is in geostrophic balance with the poleward-directed pressure gradient force and Eq.(13) pertains. Thus, rearranging,

$$v_\theta = \frac{g}{2\Omega}\frac{\partial h}{\partial r} \simeq \frac{g}{2\Omega}\frac{\Delta h}{\Delta r},$$

where Δh is the increase in the height of the 250mb surface moving outward from the pole, typically 1.5km and Δr is the lateral scale over which it occurs, typically 3000km or so. Plugging in numbers we obtain, including Earth's rotation rate and the acceleration due to gravity:

$$v_\theta = \frac{9.81\text{ms}^{-2}}{2 \times 7 \times 10^{-5}\text{s}^{-1}}\frac{(10.8 - 9.6) \times 10^3\text{m}}{3 \times 10^3\text{km}} \simeq 30\text{ms}^{-1},$$

or so, of the same order as the observed zonal wind speed — see Fig.16(top).

Connections to our radial inflow experiment should be clear. The center of our bucket represents the NP, a region of low pressure, the tilt of the free surface of the water is analogous to the tilt of atmospheric pressure surfaces, and the anti-clockwise trajectories of the paper dots are analogous and the west to east winds of the jet stream.

3.4 Extratropical cyclones and anticyclones and the gradient wind balance

As we saw, the Rossby number associated with extratropical storm is of the order one, which means that all three forces (pressure gradient, Coriolis, and centrifugal forces) are important.

We next explore in more detail how the force balance for anti-clockwise (cyclonic) and clockwise (anticyclonic) circulations (in the Northern Hemisphere, NH) can help us explain some interesting and fundamental differences between observed cyclones and anticyclones. Fig.1 below shows an example snapshot of observed sea level pressure, with 'L' and 'H' marking the centers of cyclones and anticyclones, respectively. As can be seen, cyclones are generally of smaller spatial scales and also involve much stronger pressure gradients, which also indicates stronger winds.

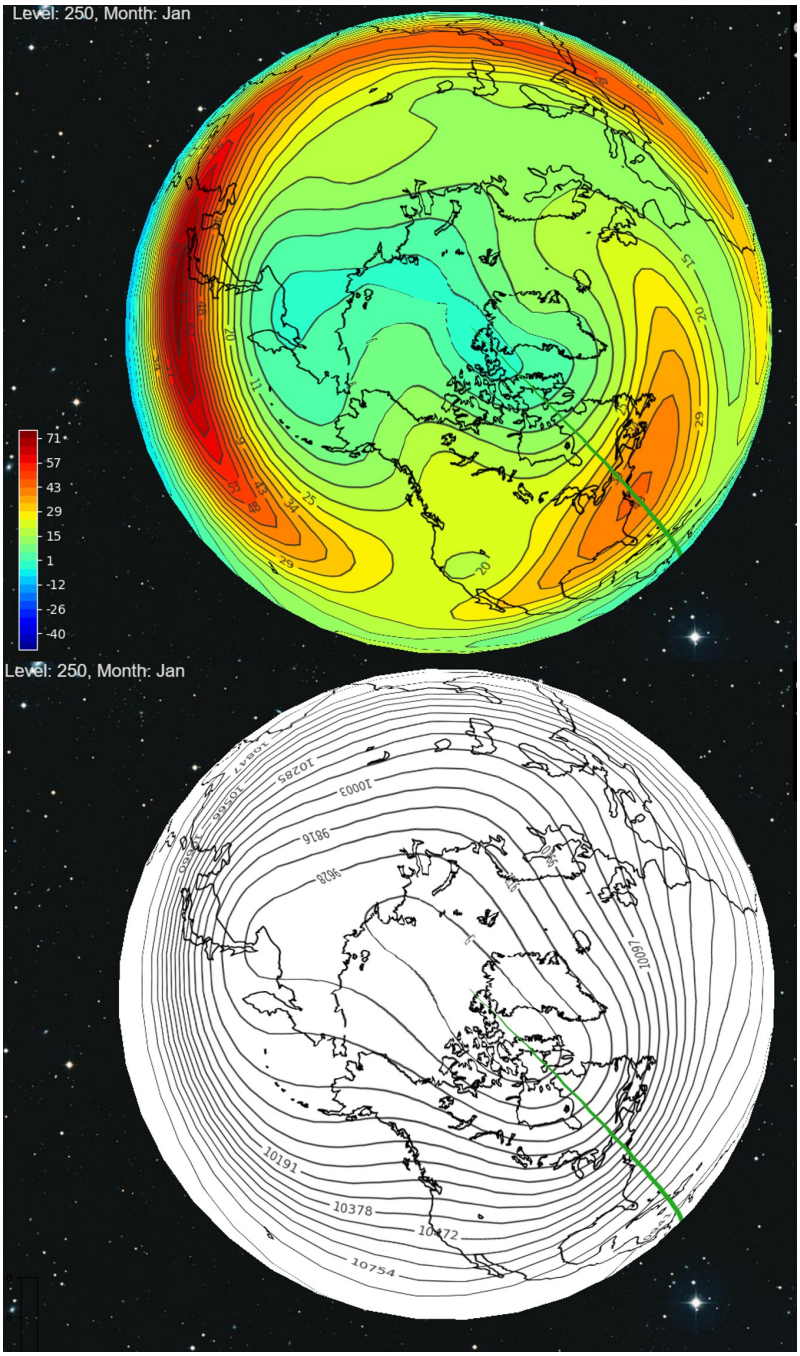

Figure 16: (top) The monthly-averaged January zonal (west to east) wind at 250mb, showing the jet stream. The north pole is in the center. Color scale on the left in ms^{-1}. Green and red colors indicate eastward flow. (bottom) The monthly-averaged January height of the 250mb surface in meters varying from a height of 9600m over the pole to10800m over the equator.

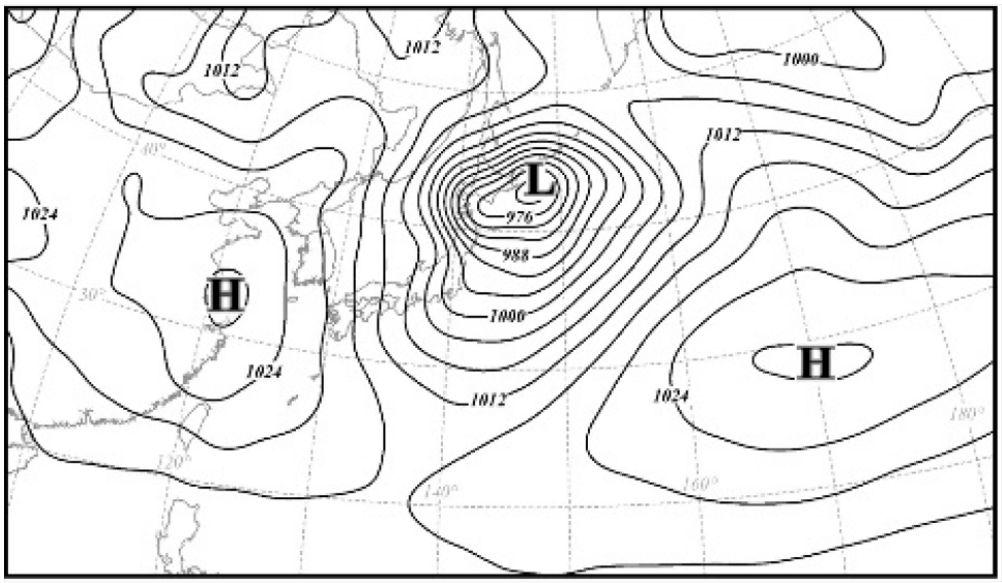

Figure 17: Sea-lavel pressure analysis for 0000 UTC 23 February 2004. Solid lines are isobars labeled in hPa and contoured every 4 hPa. Capital L and H represent centers of sea-level low- and high-pressure systems, respectively. Note the tight pressure gradient around the low and the much weaker pressure gradient around the highs. Figure taken from "Mid-Latitude Atmospheric Dynamics: A First Course" book, by Jonathan E. Martin (Figure 4.20, page 107)

To understand this, we next examine the force balance in each case.

Cyclones

For cyclones in the NH (Fig.2a), anti-clockwise circulation implies that the Coriolis force is acting outward, while the low pressure of the cyclones implies that the pressure gradient force is inwards (toward the low). The centrifugal force is outward in both cases.

The gradient wind balance is given by the equation:

$$fv_\theta + \frac{v_\theta^2}{r} = g\frac{dh}{dr} \tag{17}$$

where f is the Coriolis parameter, v_θ is the azimuthal wind speed, g is the acceleration due to gravity, h is the geopotential height, $\frac{dh}{dr}$ is the geopotential gradient, and r is the radial distance from the cyclone's center.

For cyclones, v_θ and $g\frac{dh}{dr}$ are both positive, since the rotation is anticlockwise (i.e., θ is increasing so $v_\theta = \frac{\partial\theta}{\partial t} > 0$), and the geopotential height (or similarly the pressure) is increasing outward radially.

Noting that $fv_g = g\frac{dh}{dr}$ for the geostrophic wind and plugging in (1), we find

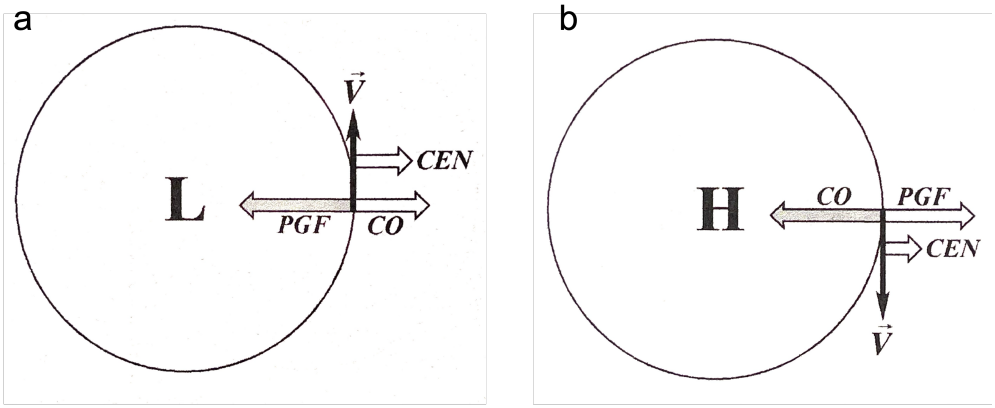

Figure 18: Force balance for a regular low 'L' (a) and regular high 'H' (b) in the Northern Hemisphere. The pressure gradient, Coriolis, and centrifugal forces are represented by PGF, CO, and CEN, respectively. Figure taken from "Mid-Latitude Atmospheric Dynamics: A First Course" book, by Jonathan E. Martin (Figure 4.17 and 4.19 on pages 104 and 106, respectively.)

$$\frac{v_\theta^2}{r} = f(v_g - v_\theta). \tag{18}$$

Now, since $\frac{v_\theta^2}{r} > 0$, it implies that $v_g > v_\theta$ for cyclones, meaning that the velocity is *subgeostrophic* i.e., smaller than the geostrophic wind.

Moreover, we can notice that (1) leads to a quadratic equation for v_θ,

$$\frac{v_\theta^2}{r} + fv_\theta - g\frac{dh}{dr} = 0,$$

whose solutions are given by the quadratic formula:

$$v_\theta = \frac{-b \pm \sqrt{b^2 - 4ac}}{2a}$$

where $a = \frac{1}{r}$, $b = f$, and $c = -g\frac{dh}{dr}$.

Hence

$$v_\theta = \frac{-f \pm \sqrt{f^2 + \frac{4}{r}g\frac{dh}{dr}}}{\frac{2}{r}} = \frac{-rf}{2} \pm \sqrt{\frac{r^2f^2}{4} + rg\frac{dh}{dr}}. \tag{19}$$

Since v_θ is positive for cyclones, the negative solution can be discarded and the overall solution is:

$$v_\theta = \frac{-rf}{2} + \sqrt{\frac{r^2f^2}{4} + rg\frac{dh}{dr}}. \tag{20}$$

Note that an additional possible mathematical solution exists where the low pressure system is rotating clockwise (as opposed to anti-clockwise), which is coined an "anomalous cyclone", but these are rarely observed in nature.

Lastly, note also that (2) implies

$$\frac{v_g}{v_\theta} = \frac{v_\theta}{fr} + 1 = R_0 + 1, \tag{21}$$

which implies that the Rossby number can be estimated using the geostrophic-to-total wind ratio.

Anticyclones

For anticyclones in the NH (Fig.2b), clockwise circulation implies that Coriolis force is acting inward, while the high pressure of the anticyclones implies that the pressure gradient force is outward (away from the high). The centrifugal force is again outward as before.

In this case, v_θ and $g\frac{dh}{dr}$ are both negative, since the rotation is clockwise (i.e., θ is decreasing so $v_\theta = \frac{\partial\theta}{\partial t} < 0$), and the geopotential height (or similarly the pressure) is decreasing outward radially. Hence, the Coriolis term and the pressure gradient terms in (1) are now both negative, while the centrifugal term $\frac{v_\theta^2}{r}$ is still positive.

In this case, (2) can be rewritten as

$$\frac{v_\theta^2}{r} = f(v_g - v_\theta) = f(|v_\theta| - |v_g|), \tag{22}$$

and since $\frac{v_\theta^2}{r} > 0$, it must be that $|v_\theta| > |v_g|$ for anticyclones, meaning that the anticyclonic wind is *supergeostrophic* i.e., larger than the geostrophic wind.

The solutions to the quadratic equation for v_θ are now

$$v_\theta = \frac{-f \pm \sqrt{f^2 - \frac{4}{r}g|\frac{dh}{dr}|}}{\frac{2}{r}} = \frac{-rf}{2} \pm \sqrt{\frac{r^2f^2}{4} - rg|\frac{dh}{dr}|}. \tag{23}$$

In this case, we notice that a solution exists only if $\frac{r^2f^2}{4} - rg|\frac{dh}{dr}| > 0$, which implies that $g|\frac{dh}{dr}| < \frac{rf^2}{4}$. This suggests that the pressure gradient of an anticyclone is bounded, and approaches zero near the center of the anticyclone. No similar constraint exists for low pressure systems, and this remarkable difference is clearly seen in sea-level pressure charts (e.g., as in Fig.1). The weak pressure gradient near the center of the anticyclone also dictates that the winds will be weak in its vicinity, as opposed to the strong cyclonic winds. [4]

[4]Note that the fact that $v_\theta < v_g$ for cyclones and $|v_\theta| > |v_g|$ for anticyclones does not imply that the anticyclone winds are stronger. This is true only for the *same pressure gradient*, which, as shown here, is

We again find that one of the solutions is unphysical and can therefore discarded, and the only physical solution is

$$v_\theta = \frac{-rf}{2} - \sqrt{\frac{r^2 f^2}{4} - rg|\frac{dh}{dr}|}. \tag{24}$$

Lastly, we also note that (6) implies in this case

$$\frac{|v_g|}{|v_\theta|} = 1 - \frac{|v_\theta|}{fr} = 1 - R_0. \tag{25}$$

Examining the gradient wind balance for real cyclones and anticyclones

We will use the Synoptic Laboratory website to plot v, v_g for real atmospheric data. Check last week- February 16th, around Washington (WA state) for a nice example.

Go to `http://synoptic.mit.edu/custom-plots/anyscalarwind/` and set:

1. In the "Scaler" field, change "tmpc" to "hght"
2. Set the day to "16" instead of today
3. In the "Wind-skip" option, change to yes (to reduce the number if arrows)
4. In the GAREA option, change "usnps" to "WA–".

This will produce a map with wind barbs and the 500mb geopotential height. Now repeat, but in the "Wind" option change "observed" to "Geostrophic".

Questions

1. Is the actual v smaller or larger than the geostrophic wind in the low and high region?
2. Can you estimate the Rossby number for each case?
3. Are winds generally stronger around the high or the low pressure?

3.5 Hurricane flow — balance of forces

We now consider hurricane flow in more detail and examine its typical balance of forces.

Theory- reminder

Radial force balance for atmospheric vortices. The radial force balance in atmospheric vorticies is very similar to the radial force balance in the radial inflow experiment. Again,

not the case.

the balance is between a pressure gradient force, a centripetal acceleration, and a Coriolis acceleration such that

$$\frac{v_\theta^2}{r} + f v_\theta = \frac{1}{\rho}\frac{\partial p}{\partial r}. \tag{26}$$

Here, v_θ is the azimuthal velocity, r is the distance from the vortex center, ρ is the density of air, and p is pressure. The main difference from the radial inflow experiment is that the Coriolis parameter is given by $f = 2\Omega \sin\phi$, where $\Omega = 2\pi/T$ is Earth's rotation rate, T is Earth's rotation period (1 day = 86400 s), and ϕ is latitude. The Coriolis parameter is modified because Earth is a rotating *sphere*, and the radial force balance in atmospheric vortices is affected by the component of the rotation vector orthogonal to Earth's surface.

Rossby Number. As for the radial inflow experiment, we can use the radial force balance to define a Rossby number

$$Ro = \frac{|v_\theta|}{fr} \tag{27}$$

that characterizes the relative magnitude of the centripetal acceleration v_θ^2/r and the Coriolis acceleration $f v_\theta$. Again, the size of the Rossby number allows us to reason about dominant terms in the radial force balance, and about whether the flow is significantly influenced by Earth's rotation.

Scatterometer data

Satellite scatterometers—instruments that use measured radar backscatter from the ocean surface to infer surface roughness and wind speed—can provide detailed maps of the near-surface wind field in hurricanes. In this assignment we will work with scatterometer data to analyze real hurricanes. Analyzing hurricane winds during the data lab will require using data from the QuickScat scatterometer instrument (which operated from 1999-2009)– so this assignment checks that you can read and plot the QuickScat data.

1. Go to the '"Weather & Extremes" Project page (→ Observation Data → scatterometer-instructions) on the course site and download qscat_20080711v4 (zip file) and one of qscathurr.m (for MATLAB users) or readscat.py (for Python users). Put all of these files in the same directory and unzip the two .gz files. (Mac users can use the Archive Utility; Windows users can use 7-Zip.) For those who prefer to work with Excel, you can also download the MATLAB script Transfer_data_to_Excel.m (which, if run after the qscathurr.m file, will convert the output the Excel sheets where you can do further analysis).

2. Run the MATLAB/Python script. It will read scatterometer data from the qscat

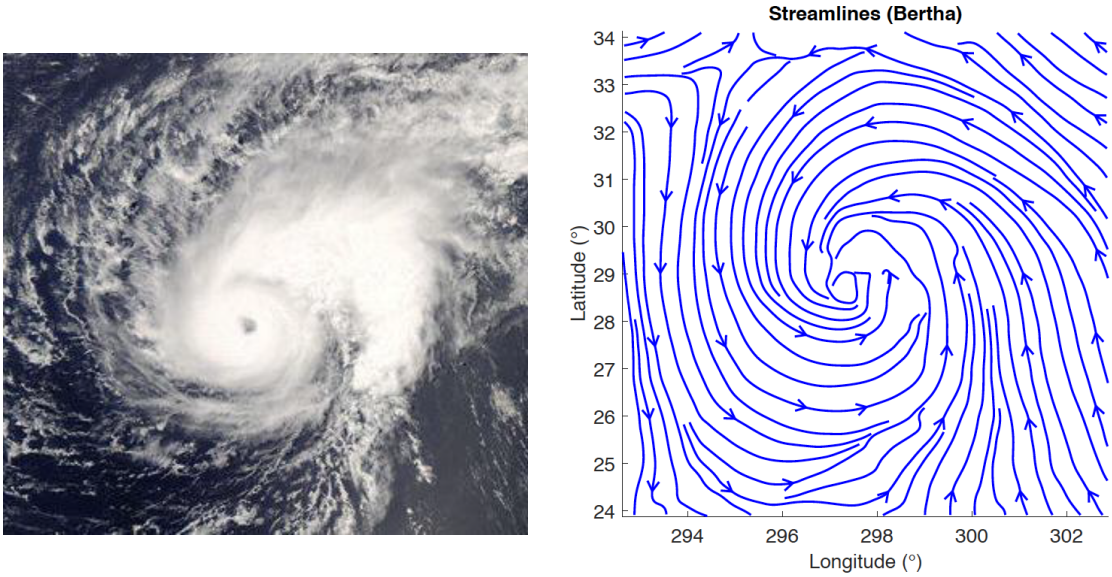

Figure 19: Satellite image of Hurricane Bertha on July 11, 2008 (left) and streamlines (trajectories of particles following the instantaneous flow) constructed from scatterometer winds for Hurricane Bertha. Scatterometer winds for Hurricane Bertha are from the QuickScat instrument on July 11, 2008.

file and plot a variety of fields centered around 29°N, 297.7°E. These should show an anti-clockwise circulation produced by Hurricane Bertha (Figure 19).

3. Investigate the plots: What does the streamline plot show? Where is the maximum wind speed? How does that value compare to typical 'everyday' winds? How does wind speed vary with radius? How about the azimuthal wind speed? Briefly comment on the contour plots of radial and azimuthal winds.

Accessing scatterometer data

Scatterometer data is available at https://www.remss.com/tropical-cyclones/storm-watch/. When searching for a hurricane to analyze, scroll down to find a list of past named storms, organized by year. Choose a hurricane case from the Storm Archive between 1999 and 2009 (recent data is not as good due to instrumentation problems). Click on the name of a storm. This will bring you to an interface for viewing scatterometer wind fields over that storm's lifetime (example in Figure 20). Finally, click on different locations in the upper bar to view scatterometer data from different days. Try to find a storm and a day where scatterometer data is available (i.e., where wind barbs are visible) over most of the region shown in the left-most panel.

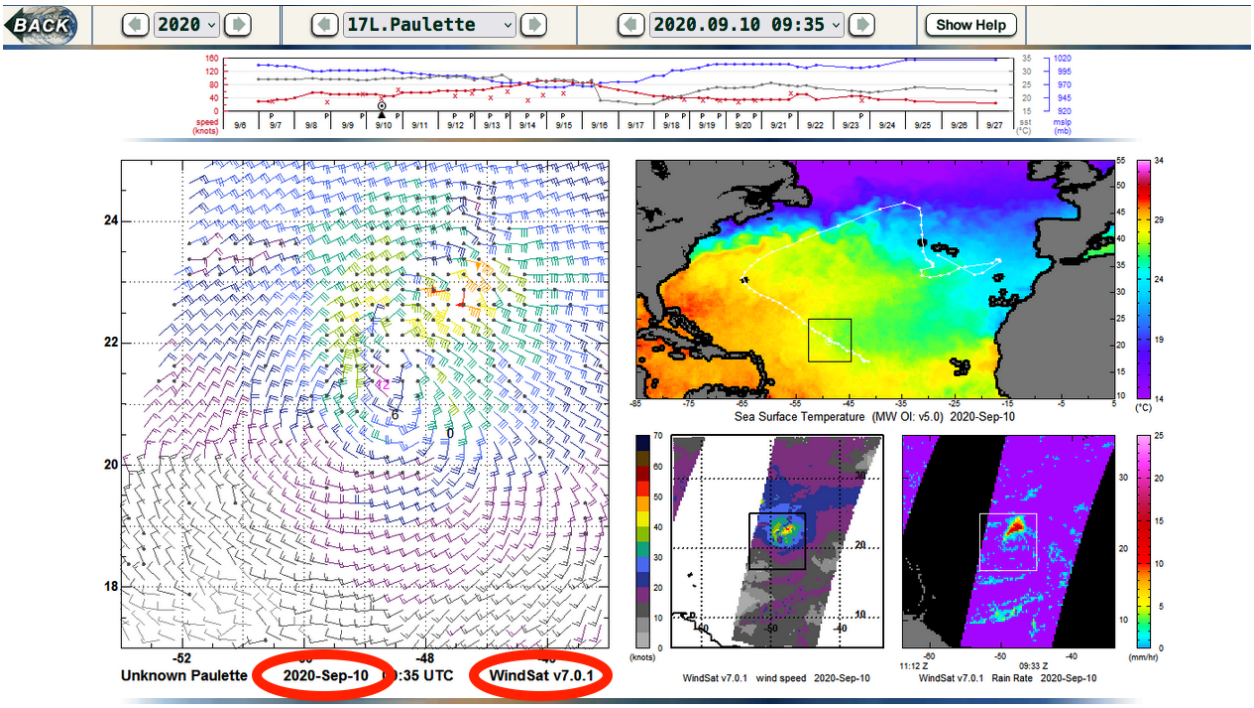

Figure 20: Interface for viewing scatterometer data from the REMSS storm archive. The scatterometer wind field is shown in the left panel, and the date and instrument are circled in red.

After finding a suitable storm, note down the year, month, day and pass of the event. Download scatterometer data from https://data.remss.com/qscat/bmaps_v04/ and unzip into your working folder. Avoid the 3 day average files (i.e., download files that end in "v4.gz", not "3day.gz").

To plot the downloaded data, you'll have to modify the `filename` variable in your Matlab/Python script to read from the right file. You'll also have to re-center plots around the center of the storm by modifying the `cntr` variable—you can estimate the approximate center from the online viewer, and tune it once you have initial plots. Finally, each file you download will contain data from two passes of the satellite, and you'll have to select the right pass by modifying the `pass` (MATLAB) or `ipass` (Python) variable so that your plots match the online viewer.

Your tasks

Analysis of hurricane wind fields.

During the data lab, you will analyze the balance of forces in hurricanes using scatterometer wind measurements.

1. Modify the readscat script to compute Rossby numbers (see section 3.5) from scatterometer data for Hurricane Bertha, and plot Rossby numbers as a function of radius.

2. Compare this plot with a prediction for the Rossby number as a function of radius based on angular momentum conservation. (Note: there's not a clear "correct" value for r_1 when analyzing hurricane winds. Instead, you should treat this value as a tunable parameter, and adjust it to see if you can obtain a good fit.)

3. Download scatterometer data for a different tropical storm (see instructions for accessing scatterometer data below) and repeat steps 1-2.

4. Discuss your results, particularly in relation to the radial inflow experiment. How does the Rossby number vary with radius, how does this compare with results from the tank experiment, and what does this imply about the balance of forces at various radii within a hurricane? Does theory based on angular momentum conservation predict $Ro(r)$ equally accurately for the lab experiment and the hurricane, and if not, why might that be?